

# Early Warnings for Multistage Transitions in Dynamics on Networks

Neil G. MacLaren<sup>1</sup>, Prosenjit Kundu<sup>1,†</sup>, and Naoki Masuda<sup>1,2\*</sup>

<sup>1</sup>*Department of Mathematics, State University of New York at Buffalo, NY 14260-2900, USA*

<sup>2</sup>*Computational and Data-Enabled Science and Engineering Program,*

*State University of New York at Buffalo, Buffalo, NY 14260-5030, USA and*

<sup>†</sup>*Present address: Dhirubhai Ambani Institute of Information and*

*Communication Technology, Gandhinagar, Gujarat 382007, India.*

(Dated: March 2, 2023)

Successfully anticipating sudden major changes in complex systems is a practical concern. Such complex systems often form a heterogeneous network, which may show multistage transitions in which some nodes experience a regime shift earlier than others as an environment gradually changes. Here we investigate early warning signals for networked systems undergoing a multistage transition. We found that knowledge of both the ongoing multistage transition and network structure enables us to calculate effective early warning signals for multistage transitions. Furthermore, we found that small subsets of nodes could anticipate transitions as well as or even better than using all the nodes. Even if we fix the network and dynamical system, no single best subset of nodes provides good early warning signals, and a good choice of sentinel nodes depends on the tipping direction and the current stage of the dynamics within a multistage transition, which we systematically characterize.

Keywords: complex networks; early warning signals; critical transitions; tipping points; dynamics on networks

## I. INTRODUCTION

A characterization of complex systems is dependence among components, which often leads to surprising, nonlinear behavior. One important nonlinear phenomenon is that of a tipping point: a transition in which stable aspects of the system suddenly shift to a drastically altered state when the system's environment changes by a small amount; recovery from the altered state is typically difficult. Tipping points have been described in, for example, the switch from clear to turbid water in lake ecosystems [1], changes in fish community composition [2], alterations in global climate regimes [3], and in the progression of disease [4, 5]. This shared feature of such disparate systems can be described mathematically by bifurcations, and several early warning signals—statistical

---

\* Correspondence: naokimas@buffalo.edu

31 indications that a bifurcation point is nearby—have been developed that attempt to anticipate such  
32 transitions. These early warning signals rely on a process called critical slowing down: systems  
33 recover from perturbations more slowly near a bifurcation point [6]. Critical slowing down results  
34 in predictable signatures in time series data, including increasing variance and autocorrelation,  
35 and it is these signatures that are used to construct early warning signals. Early warning signals  
36 based on the critical slowing down phenomenon have been validated in several model systems [2, 7],  
37 and their practical utility has been demonstrated in, e.g., predicting electrical grid failures [8] and  
38 reversing cyanobacterial blooms [9].

39 Many systems showing tipping points can be modeled by a network in which a node represents  
40 a dynamical system and different dynamical systems interact through the edges of the network  
41 [10]. Studying tipping points in such systems is an integral part of studying network robustness  
42 and resiliency [11]. An example with applications in conservation ecology is the anticipation of  
43 a breakdown in mutualistic species networks [12–14]. In such models, species populations are  
44 typically represented by stochastic differential equations interacting through a bipartite network  
45 of plants and pollinators [15, 16] or a unipartite projection focusing on only plants or pollinators  
46 [12, 17]. Early warning signals can then predict major adjustments in species composition [12] or  
47 population collapse [14]. Similarly, exploiting information on interactions between weather patterns  
48 in different regions may improve the forecasting of climate tipping points [18].

49 In fact, the inherent heterogeneity in networked systems may make tipping points more complex.  
50 Specifically, multistage transitions, in which not all components transition to an alternate state at  
51 the same parameter values, may be the rule rather than the exception in networks with certain  
52 features [19, 20]. Multistage transitions have been documented in studies of mutualistic species  
53 dynamics [12, 14] and climate systems [18], and are consistent with evidence from human commensal  
54 bacteria [21] and social upheaval [22]. The ability to anticipate multistage transitions would thus  
55 have applications in many fields.

56 A variety of methods have been proposed to provide early warning of tipping points on networks.  
57 Examples include aggregations of univariate (i.e., single-node) early warning signals and explicitly  
58 multivariate methods such as measures derived from a principal component analysis (PCA) of  
59 state variables [11, 23]. However, most of the available early warning signals for networks treat the  
60 network as a united entity and do not exploit the fact that a network is composed of subsystems  
61 that may show different dynamics and provide different early warning signals. There are some  
62 notable exceptions. First, Chen et al. used cross-correlations to identify clusters of nodes that  
63 were more sensitive to an approaching bifurcation than the network as a whole [24]. Although

64 Chen et al. exploited network heterogeneity for constructing early warning signals, they did not  
 65 consider multistage transitions. Second, Lever et al. developed PCA methods to predict the  
 66 direction and magnitude of change for each node’s state after a bifurcation [12]. Lever et al.  
 67 noted parameter ranges for their model in which multistage transitions were possible and that the  
 68 early warning signal they proposed tended to correctly anticipate the first transition. However,  
 69 Lever et al. noted that their method was less reliable for describing further nodes’ transitions—  
 70 the multistage transition. Third, Aparicio et al. used network control theory—rather than system  
 71 dynamics—to identify nodes that would be capable of providing a reliable early warning signal [14].  
 72 They also identified parameter values that caused multistage transitions in their model and also  
 73 found that their method underperformed in those regions. In contrast to Lever et al.’s method,  
 74 Aparicio et al.’s method tended to miss early transitions of nodes but correctly predicted the final  
 75 collapse. Based on the ubiquitousness of multistage transitions in networks, discussed above, there  
 76 is a need for early warning signals that can provide alerts for each of the major tipping points  
 77 within a multistage transition that a networked system may experience.

78 In the present study, we build on key points from these three studies—namely that (1) some  
 79 nodes may be more informative about impending transitions than others and (2) information may  
 80 be available in the network structure or dynamics with which to anticipate multistage transitions—  
 81 to investigate early warning signals for multistage transitions in tipping dynamics on networks. We  
 82 find that traditional early warning signals are in fact able to provide early warning in a network  
 83 undergoing a multistage transition. Using knowledge of the network allows us to choose “sentinel”  
 84 nodes, i.e., node sets that can provide early warning more efficiently than using all nodes in terms  
 85 of the number of nodes we must observe. Furthermore, it is often the case that such early warning  
 86 signals even improve in accuracy.

## 87 II. METHODS

### 88 A. Model

89 Consider an undirected and unweighted network of  $N$  nodes and denote its adjacency matrix  
 90 by  $A = (a_{ij})$  with  $a_{ii} = 0$  and  $a_{ij} = a_{ji} \in \{0, 1\} \forall i, j \in \{1, \dots, N\}$ . We simulate the stochastic  
 91 dynamics of a coupled double-well model on networks given by

$$\frac{dx_i}{dt} = -(x_i - r_1)(x_i - r_2)(x_i - r_3) + D \sum_{j=1}^N a_{ij} x_j + s\xi_i, \quad (1)$$

92 where  $x_i$  is the state of node  $i$ ;  $r_1$ ,  $r_2$ , and  $r_3$  are parameters that control the location of the  
 93 equilibria and satisfy  $r_1 < r_2 < r_3$ ;  $D$  ( $\geq 0$ ) is the coupling strength; and  $s\xi_i$  is a Gaussian noise  
 94 process with standard deviation  $s$ . The first term is the derivative of a fourth-order polynomial  
 95 representing a double-well potential. In the uncoupled and noiseless case, it produces lower and  
 96 upper stable equilibria at  $x_i = r_1$  and  $x_i = r_3$ , respectively, and an unstable equilibrium at  $x_i = r_2$ ,  
 97 and it also creates hysteresis. Unless we state otherwise, we set  $(r_1, r_2, r_3) = (1, 4, 7)$ . The coupling  
 98 term  $D \sum_{j=1}^N a_{ij}x_j$  shifts  $x_i$  at the stable equilibria out of  $x_i = r_1 = 1$  or  $x_i = r_3 = 7$ . In addition,  
 99 the noise term  $s\xi_i$  lets  $x_i$  jitter around the stable equilibria obtained in the absence of noise. We  
 100 therefore consider that nodes with  $x_i < 2.268$  are in the lower state and  $x_i > 2.268$  are in the upper  
 101 state. We selected this threshold value for  $x_i$  because the cubic term in Eq. (1) has an inflection  
 102 point at  $x_i \approx 2.268$  in the absence of the coupling term, demarcating a basin of attraction for  
 103 the lower stable point at  $x_i = 1$ . We numerically verified that we can reliably classify  $x_i$  into the  
 104 lower and upper stable equilibria with these threshold values even in the presence of the coupling  
 105 term (see Figure S1). Equation (1) represents dynamics of species abundance [12] or climates  
 106 in interconnected regions [18]. We primarily consider  $D$  as a bifurcation parameter. A possible  
 107 mechanism underlying variation in  $D$  is the volume of moisture moving from one climate basin to  
 108 another [18].

109 For applications such as species loss in population ecology, one is interested in beginning with  
 110 the upper state, which corresponds to the situation in which all the species are abundant, and  
 111 gradually varying a parameter value to anticipate transitions of various nodes to their lower states  
 112 [6]. For example, a transition to the lower state could correspond to the collapse of a species'  
 113 population. To validate the relevance of multistage transitions and early warning signals in this  
 114 scenario, we consider an extension of Eq. (1) given by

$$\frac{dx_i}{dt} = -(x_i - r_1)(x_i - r_2)(x_i - r_3) + D \sum_{j=1}^N a_{ij}x_j + u + s\xi_i. \quad (2)$$

115 Variable  $u$  is a stressor that directly and uniformly influences all nodes. An increase in  $u$  repre-  
 116 sents, for example, increased global mean temperature [18] or degradation of the local environment  
 117 causing increased mortality for all species [12]. With Eq. (2), we hold either  $D$  or  $u$  constant and  
 118 vary the other as the bifurcation parameter.

## B. Numerical Simulations

Unless we state otherwise, we used  $D$  as the bifurcation parameter and began simulations with all nodes in the lower state. For the given network and the value of  $D$ , we started the dynamics from the initial condition  $x_1 = \dots = x_N = 1$ . For any given value of  $D$ , we integrated Eq. (1) using the Euler-Maruyama method with time step  $\Delta t = 0.01$  for 50 time units (TU) to allow  $\{x_1, \dots, x_N\}$  to relax to an equilibrium. In fact, allowing 50 TU was sufficient except in rare cases in which some nodes changed their macroscopic state (i.e., lower versus upper state) after 50 TU due to dynamical noise. We then continued simulating the dynamics for a further 25 TU to take samples from  $\{x_1(t), \dots, x_N(t)\}$  for calculating early warning signals. We used  $s = 0.05$  except where noted.

To determine whether or not early warning signals increase prior to transitions of various nodes from their lower state to upper state, we conducted sequences of the above simulations for a given network and set of parameters. Each sequence began with  $D = 0.01$ . After we simulated the dynamics for 75 TU in total and calculated early warning signals, we increased  $D$  by 0.005, reset  $x_i \forall i$  to the initial condition, ran the simulation with the new value of  $D$ , and calculated early warning signals from the new  $x_i(t)$ . We continued this procedure (i.e., increasing  $D$  by 0.005 and running a new simulation) until at least 90% of nodes reached the upper state at equilibrium.

In simulations with  $D$  as the bifurcation parameter but with the nodes beginning in the upper state, we set  $x_i = 7 \forall i$  and  $u = -15$ . In this case, we consider that nodes with  $x_i < 5.732$  are in the lower state and  $x_i > 5.732$  are in the upper state; note that Eq. (1) has a second inflection point at  $x_i \approx 5.732$  in the absence of the coupling term. We initially set  $D = 1$  and decreased  $D$  by 0.005 in each simulation, continuing until  $> 90\%$  of nodes transitioned to the lower state at equilibrium. All other parameters were the same regardless of whether we began simulations with the nodes at the upper or lower state.

This simulation method attempts to ensure that we always study the system at equilibrium and has been used in previous studies of tipping points on networks (e.g., [18]). De-trending or other preprocessing of data from the simulations is therefore not needed: by the time we take data from each simulation, the system is stationary by design (c.f. [25] for a different simulation method, for which de-trending is required).

148

### C. Early Warning Signals

149 At each value of  $D$ , we calculated the following early warning signals [23, 25] from  $M = 250$   
 150 equally spaced samples of  $\{x_1(t), \dots, x_N(t)\}$  with  $t \in (50, 75]$ , i.e., with  $t \in \{50.1, 50.2, \dots, 75.0\}$ :

- 151 • The dominant eigenvalue  $\lambda_{\max}$  of the covariance matrix, of which the  $(i, j)$  entry is the  
 152 covariance of  $\{x_i(50.1), x_i(50.2), \dots, x_i(75)\}$  and  $\{x_j(50.1), x_j(50.2), \dots, x_j(75)\}$ .
- 153 • The standard deviation of each  $x_i(t)$  estimated from the  $M$  samples.
- 154 • The lag-1 autocorrelation of each  $x_i(t)$ , defined as  $\frac{\sum_{m=1}^{M-1} (x_{i,m} - \bar{x}_i)(x_{i,m+1} - \bar{x}_i)}{\sum_{m=1}^M (x_{i,m} - \bar{x}_i)^2}$ , where  $x_{i,m} \equiv$   
 155  $x_i(50 + 0.1m)$  and  $\bar{x}_i = \sum_{m=1}^M x_{i,m}/M$ .

156 To define an early warning signal for a given node set, we used both the maximum and the mean  
 157 of the standard deviation and lag-1 autocorrelation in addition to  $\lambda_{\max}$  calculated from the node  
 158 set of interest. Therefore, we examine five different early warning signals for a given set of nodes  
 159 (see section IID for the node sets).

160 We quantify the extent to which an early warning signal anticipates a bifurcation with the  
 161 Kendall rank correlation,  $\tau$ , between  $D$  before the bifurcation occurs and the early warning signal  
 162 [26]. The reasoning behind using Kendall's  $\tau$  as a performance metric is as follows. Consider a  
 163 range of  $D$  in which no nodes change state at equilibrium except at the final value of  $D$ . We refer  
 164 to a range of  $D$  in which the number of nodes in the lower/upper state is constant as a stable range.  
 165 Given our simulation protocol,  $D$  is linearly increasing in a stable range. If an early warning signal  
 166 tends to increase as  $D$  increases towards the bifurcation point, indicating critical slowing down,  
 167 then the early warning signal is considered to be useful in anticipating the bifurcation, and  $\tau$  tends  
 168 to be large. However, in the network dynamics that we are considering, there are potentially many  
 169 values of  $D$  at which some nodes switch from the lower to the upper state. Therefore, we correlate  
 170  $D$  with a given early warning signal to obtain  $\tau$  only within stable ranges of  $D$  having at least 15  
 171 unique values of  $D$ . We report the  $\tau$  value averaged over all such stable ranges. For example, if  
 172 there is no node transitioning from its lower state to the upper state for  $D \in \{0.01, 0.015, \dots, 0.5\}$ ,  
 173  $D \in \{0.505, 0.51, 0.515\}$ , and  $D \in \{0.52, 0.525, \dots, 1\}$ , some nodes transit from the lower to the  
 174 upper state at  $D = 0.505, 0.52$ , and  $1.005$ , and the transition at  $D = 1.005$  makes the fraction of  
 175 the nodes in the upper state exceed 0.9, then we calculated  $\tau$  for the first and third ranges of  $D$   
 176 and took the average of the two  $\tau$  values.

## D. Node Sets

177

We defined the following nine node sets for calculating the early warning signals:

178

179

- “All” refers to the set of all nodes.

180

- “Lower State” refers to the set of all nodes in the lower state at  $t = 50$  TU.

181

- “Upper State” refers to the set of all nodes in the upper state at  $t = 50$  TU. If there are no nodes in the upper state, this node set is empty and early warning signals for this node set are undefined.

182

183

184

- “High Input” refers to the  $n$  nodes that are largest in terms of  $R_i = \sum_{j=1}^N a_{ij} \bar{x}_j$ , where  $i$  is the index of an available node in the sense that it is still in its original macro state. For example, a lower-state node is an available node if nodes are initially in the lower state in a simulation. Note that such a node is available to transition to the upper state as  $D$  increases. We remind that  $\bar{x}_j$  is the mean of  $x_j$  calculated over the  $M$  samples. We define the High Input node set based on the idea that a lower-state node with many neighbors or with neighbors in the upper state is more likely to transition from the lower to the upper state earlier than other nodes.

185

186

187

188

189

190

191

192

- “Low Input” refers to the  $n$  nodes that are the smallest in terms of  $R_i$ . As for High Input, we require that the  $i$ th node is in its original macro state. The Low Input node set reflects the observation that, if the nodes are initially in the upper state, then the node with the smallest contribution from the coupling term, i.e., those with smallest  $R_i$ , would be the first to transition to the lower state as  $D$  decreases.

193

194

195

196

197

- “Lower Half” refers to the set of lower-state nodes below the median in terms of  $R_i$ ; we do not use this node set when all the nodes are initially in the upper state in the simulation. If the nodes begin in the lower state, Lower Half nodes are the farthest from a bifurcation as one gradually increases  $D$ .

198

199

200

201

- “Random” refers to the set of  $n$  nodes selected uniformly at random.

202

203

204

205

- “Large Correlation” nodes are the top  $n$  nodes in terms of  $R'_i = \sum_{j=1; j \neq i}^N \text{cor}(x_i, x_j) \bar{x}_j$ , where the  $i$ th node is a lower-state node, and  $\text{cor}(x_i, x_j)$  is the Pearson correlation coefficient between  $x_i$  and  $x_j$  calculated over the  $M$  samples. This is an alternative for High Input when we do not have access to the network structure, i.e., the adjacency matrix.

206 • “Large Standard Deviation (Large SD)” nodes are the  $n$  nodes with the largest standard  
 207 deviation of  $x_i$  over the  $M$  samples. A node tends to have a larger standard deviation when  
 208 it receives a larger input from the coupling term. Thus, the Large SD node set is also an  
 209 alternative for High Input when we do not have information about the network structure.

210 The All node set corresponds to established early warning signal methods and is the most costly in  
 211 terms of sampling effort. The High Input, Low Input, Random, Large Correlation, and Large SD  
 212 node sets require a limited number of nodes, which we set  $n = 5$ , and are therefore the least costly.  
 213 The other node sets are variable in terms of the number of nodes. However, with the exception of  
 214 the first stable range, the number of nodes used is typically much larger than  $n$  and much smaller  
 215 than  $N$  across a wide range of  $D$ . All, Lower State, Upper State, Random, Large Correlation, and  
 216 Large SD do not use the information on the network structure, whereas High Input, Low Input,  
 217 and Lower Half do. Random, Large Correlation, and Large SD are most economic in the sense that  
 218 it only uses  $n$  nodes and does not require the network structure. We updated node set membership  
 219 each time we change the value of  $D$ .

220

### E. Networks

221 We conducted simulations on 6 model networks and 17 empirical networks; see the Supple-  
 222 mentary Information (SI) for details of the networks. We chose networks having the order of 100  
 223 nodes, similar in size to many empirical networks and small enough to be computationally feasible  
 224 for our simulations. We chose model networks with a range of degree heterogeneities and with and  
 225 without a planted community structure, including networks that show a multistage transition to  
 226 different extents [20]. Empirical networks may have a variety of features difficult to capture with  
 227 model networks and thus present hidden challenges to our methods. An example of our empirical  
 228 networks is a dolphin social network [27]. In this network, the nodes are individual dolphins and  
 229 two nodes are adjacent if individuals  $i$  and  $j$  were observed together more often than expected  
 230 by chance. On such a network,  $x_i$  represents, for example, a behavioral state or possession of  
 231 particular information.

232

### F. Robustness Analysis

233 We tested several variations of our methods to examine robustness under different scenarios.  
 234 First, to test the robustness of these results with respect to the network structure, we conducted



235 simulations on the 23 networks explained in Section II E. Ten of the 23 networks had at least two  
 236 stable ranges, showing clear multistage transitions. We selected these ten networks for further  
 237 analysis.

238 Consider an early warning signal. On each of the ten selected networks, we calculated  $\tau$  between  
 239 the early warning signal and  $D$  for each stable range of  $D$ . We then averaged  $\tau$  over the stable  
 240 ranges of  $D$ . We calculated such an averaged  $\tau$  value 50 times, restarting simulations with a new  
 241 random seed each time, for each of the three node sets (i.e., All, Lower State, and High Input) and  
 242 each network. Finally, we estimated a linear mixed effects model to predict the averaged  $\tau$  value  
 243 based on three levels of a node-set fixed effect variable (i.e., All as the reference, Lower State, and  
 244 High Input) with a random effect for network. We estimated the linear mixed effects model in this  
 245 manner for each of the five early warning signals.

246 Second, we varied several simulation parameters on two arbitrarily selected networks. The  
 247 adjusted parameters were the noise intensity ( $s \in \{0.01, 0.1, 0.5\}$ ), the number of samples taken  
 248 from each  $x_i(t)$  when calculating early warning signals ( $M \in \{25, 50, 150\}$ ), the double-well model  
 249 parameters ( $(r_1, r_2, r_3) \in \{(1, 3, 5), (1, 2.5, 7), (1, 5.5, 7)\}$ ), and the duration  $T$  of the simulation  
 250 before we start to sample  $\{x_1(t), \dots, x_N(t)\}$  to calculate the early warning signals at each value of  
 251  $D$  ( $T \in \{25, 75, 100\}$ ).

252 Third, we altered the model itself, examining transitions from the upper to the lower state using  
 253 Eq. (2).

254

## G. Software

255 We conducted all simulations and analyses in R (v4.2); dependencies include the “igraph”  
 256 package (v1.3) for network analysis [28], the “nlme” package (v3.1) for mixed effects statistical  
 257 models [29], and the “parallel” package (v4.2) [30] for parallel processing. Empirical networks  
 258 were drawn from the “networkdata” package [31]. Code and data to reproduce these analyses are  
 259 available at <https://github.com/ngmaclaren/doublewells>.

### III. RESULTS

#### A. Multistage Transitions and Performance of Early Warning Signals Based on Different Node Sets

Let us first consider a network with 100 nodes and a power-law degree distribution generated by a configuration model, which we call the power-law network. We show by the gray line in Figure 1A the proportion of nodes in the lower state in the equilibrium as a function of the coupling strength between nodes,  $D$ . The figure shows that more nodes tend to be in the upper state in the equilibrium when  $D$  is larger. Additionally, there are ranges of  $D$  in which relatively large changes in  $D$  do not induce transition of any node from the lower to the upper state at equilibrium. In other ranges of  $D$ , small changes in  $D$  trigger transitions of some nodes between macro states. In this manner, the noisy double-well model on this network shows a multistage transition. We also find a multistage transition when we use Eq. (2) and vary  $u$  instead of  $D$  as the bifurcation parameter (Fig. S2).

Early warning signals appear to be sensitive to changes in  $D$ . Figure 1A also shows a typical early warning signal, i.e., the lag-1 autocorrelation of  $x_i(t)$ , averaged over three different node sets. The first, “All” (black), corresponds to traditional early warning signals and refers to the set of all nodes. Within the stable ranges of  $D$ , the early warning signal value tends to increase as  $D$  increases. However, different nodes may be differently informative as to an impending transition. Both observed dynamics [12, 24] and knowledge of network structure [14] may improve the accuracy of early warning signals or their efficiency in terms of the amount of observed signals necessary for the calculation. In fact, it may be more efficient to monitor nodes that are most likely to transition to an alternate state with a perturbation of a control parameter.

To show that monitoring sentinel node sets can be effective, Figure 1A also displays the early warning signal calculated for the set of nodes in the lower state at  $t = 50$  TU (“Lower State”, red) and the set of five nodes most likely to transition from the lower to upper state (“High Input”, green). These latter nodes have many neighbors, are connected to nodes that have transitioned to the upper state, or both; they have the highest value of  $R_i \equiv \sum_{j=1}^N a_{ij} \bar{x}_j$  by definition. Figure 1A shows that the sensitivity of the average autocorrelation to the increase in  $D$  towards the end of a stable range varies depending on the node set and the value of  $D$ . For example, there is a major sudden increase in the number of nodes in the upper state at equilibrium at  $D = 0.95$ . This transition is associated with, looking from left to right, a marked increase in the average

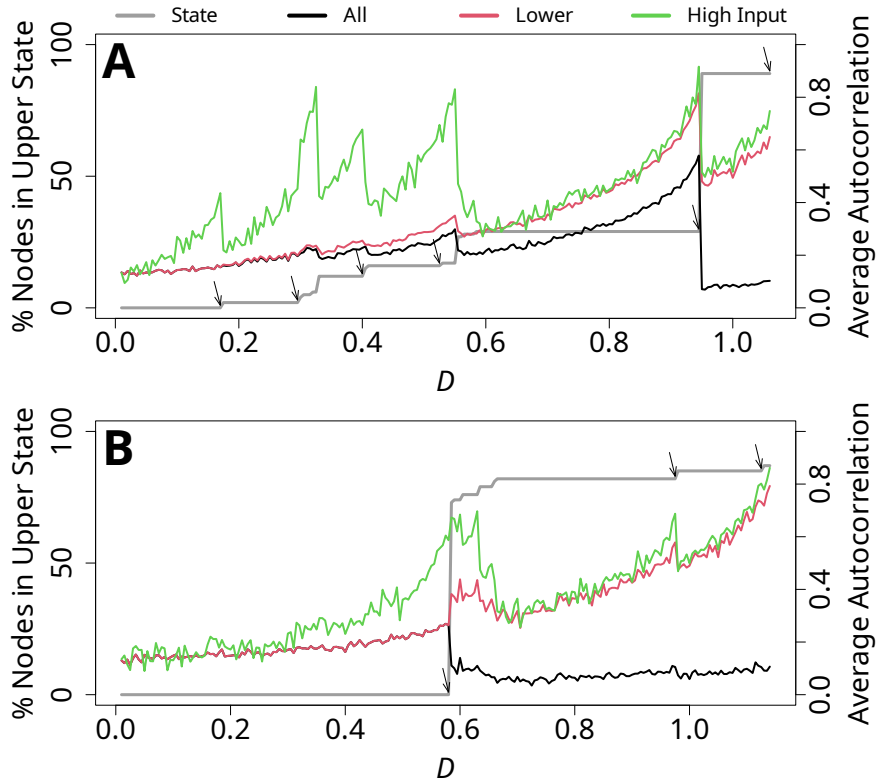


FIG. 1. Multistage transitions when the nodes are initially in the lower state. We show the number of nodes in the upper state at equilibrium (gray), and the average lag-1 autocorrelation of  $x_{i,t}$  calculated for all nodes (black), the nodes in the lower state (red), and the low-input nodes (green). The arrows mark transitions of some nodes at the ends of stable ranges. (A) A network with 100 nodes and a power-law degree distribution; (B) Dolphin social network.

291 autocorrelation of the nodes in each of the node sets at  $D$  just below 0.95 and a decrease in the  
 292 average autocorrelation at  $D = 0.95$ . A similar tendency is present around the transitions of  
 293 smaller batches of nodes at, for example,  $D = 0.175$ ,  $0.33$ , and  $0.55$ . Changes in the average  
 294 autocorrelation of the High Input nodes tend to be larger in absolute value than for the Lower  
 295 State and All node sets, particularly at smaller values of  $D$ , but the overall range is similar in this  
 296 network.

297 Figure 1B shows that the double-well model on a dolphin social network [27] also exhibits a  
 298 multistage transition. See Fig. S2 for similar results when  $u$  is the bifurcation parameter. Compared  
 299 to the case of the power-law network, the dolphin network allows larger stable ranges of  $D$ , and  
 300 the ranges of  $D$  in which small changes in  $D$  induce a transition of a notable fraction of nodes  
 301 from the lower to the upper state are narrower. Similar to Fig. 1A, the autocorrelation tends to  
 302 reliably increase in each stable range of  $D$  as we increase  $D$  towards the value at which some nodes

303 transit from the lower to the upper state. In addition, the average autocorrelation based on the  
 304 Lower State and High Input node sets apparently better signals such transitions than that based  
 305 on all nodes in the sense that the average autocorrelation increases more drastically as  $D$  increases  
 306 towards the bifurcation.

307 To quantify the performance of the average autocorrelation and other early warning signals, we  
 308 computed the Kendall's  $\tau$  for each of the two networks used in Fig. 1 and for each of the five early  
 309 warning signals calculated for each node set. We show the results in Fig. 2, which indicates that  
 310  $\tau$  is high (i.e.,  $> 0.65$ ) across both networks and all five early warning signals and for All (circles),  
 311 Lower State (triangles), and High Input (pluses) node sets. The  $\tau$  values for each early warning  
 312 signal in both networks are similar between Lower State and High Input, and they are higher than  
 313 for All in a majority of cases. In addition to having a high average  $\tau$  value, the High Input node  
 314 set has  $\tau > 0.7$  for each major transition in both networks (see SI section S4 and Fig. S6 for  
 315 details). If we calculate the average autocorrelation for the nodes that actually changed state at  
 316 each major transition, we of course find that the  $\tau$  value for this retroactively identified node set  
 317 is high. However, the High Input node set has almost the same performance, in terms of  $\tau$  at each  
 318 transition, as the nodes that actually changed state (Fig. S6). Furthermore, by definition, early  
 319 warning signals calculated with the Lower State and High Input node sets are more cost-efficient  
 320 than those calculated with all nodes because the former use only a fraction of nodes. However, our  
 321 typical simulations use samples of  $x_i$  at all  $M$  time points for both assigning nodes to node sets  
 322 and calculating early warning signals. We performed additional simulations, described in section  
 323 S5, which only used the samples at the first ten time points to determine node set membership.  
 324 We then monitored the node set members for the full  $M$  samples including the first ten samples  
 325 for calculating early warning signals. Our results are robust to this decision, as we show in Fig. S7.  
 326 Finally, the High Input node set performs well even when we consider all node transitions, not just  
 327 those occurring after a stable range (Fig. S8).

328 Although the Lower State node set is both more accurate and efficient than the set of all nodes,  
 329 this result does not imply that any nodes in the lower state provide a good early warning signal.  
 330 To show this, we investigated early warning signals constructed from half of the lower-state nodes  
 331 whose  $R_i$  score is the lowest—those with relatively few neighbors or few neighbors in the upper  
 332 state. This node set, termed “Lower Half” and shown by the diamonds in Fig. 2, typically yielded  
 333 lower  $\tau$  values than the All, Lower State, and High Input node sets. This result implies that one  
 334 needs to assemble an early warning signal from carefully chosen lower-state nodes such as those  
 335 with large  $R_i$  values. Finally, Upper State (shown by the crosses in Fig. 2) and Random (shown

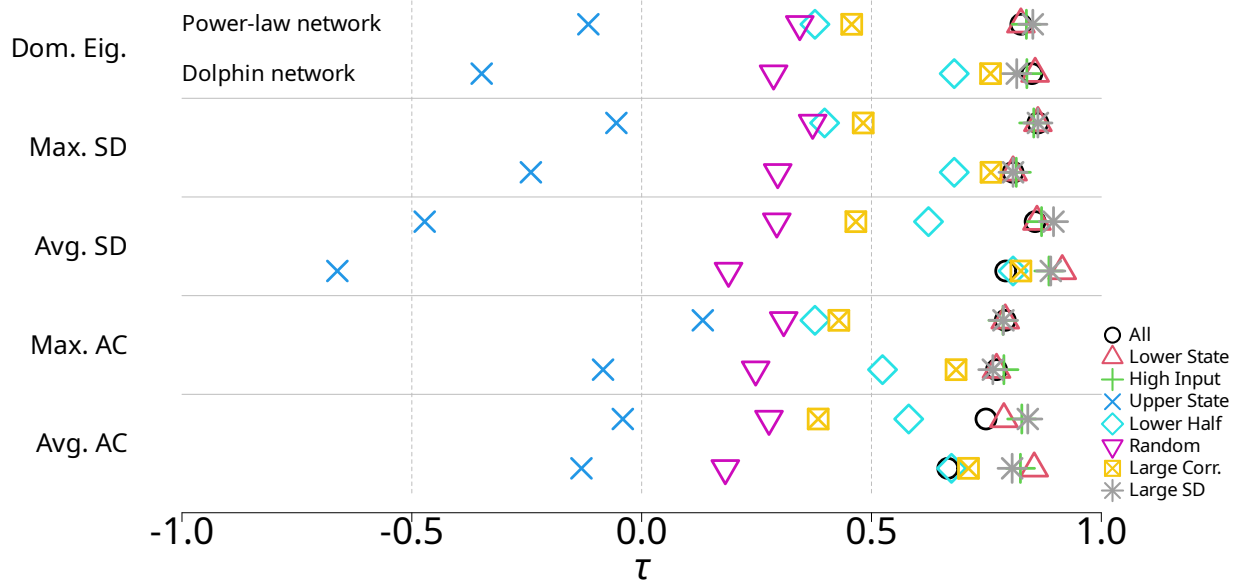


FIG. 2. Kendall correlations ( $\tau$ ) between each of the five early warning signals and the coupling strength,  $D$ , for different sets of nodes. See main text for details of node set membership. Dom. Eig: dominant eigenvalue of the covariance matrix of all nodes in the node set, Max. SD, Avg. SD: maximum and average standard deviation of  $x_i$ , Max. AC and Avg AC: maximum and average autocorrelation of  $x_i$ , Large Corr.: the Large Correlation node set.

336 by the inverted triangles) node sets are either negatively correlated or not correlated with  $D$ ,  
 337 reinforcing our claim that the choice of nodes to be observed is essential. In sum, our simulation  
 338 results suggest that, with a proper choice of observed node set—including the case of observing  
 339 all nodes—standard multivariate and aggregated univariate indicators reliably increased in value  
 340 prior to several transitions of nodes from the lower to upper state, performing well throughout a  
 341 multistage transition.

## 342 B. Robustness against Variation in Networks and Parameter Values

343 To quantitatively examine the dependence of  $\tau$  on network structure, we constructed a linear  
 344 mixed effects model explaining  $\tau$  with a fixed effect of node set and a random effect of network  
 345 (Fig. 3; see section S9 for the statistical results). We found that the predicted  $\tau$  is large (i.e.,  
 346 approximately larger than 0.75) across most networks, early warning signals, and node sets; the  
 347 combination of the All node set and the average autocorrelation early warning signal yielded a  
 348 somewhat lower predicted  $\tau$  value (i.e., 0.667). Variance-based methods (i.e., dominant eigenvalue

349 and the maximum and average node-level standard deviation) tended to produce higher predicted  
 350  $\tau$ , ranging between 0.792 and 0.828. The autocorrelation methods produced lower predicted  $\tau$ ,  
 351 ranging between 0.667 and 0.766, although these values were still relatively high compared to  
 352 other published results (e.g., [25, 26]). The early warning signals based on the Lower State nodes  
 353 were either no different (dominant eigenvalue,  $p = 0.050$ ; maximum standard deviation,  $p = 0.173$ ;  
 354 and maximum autocorrelation,  $p = 0.290$ ; uncorrected for multiple comparison) or better (average  
 355 standard deviation,  $p < 10^{-4}$ ; and average autocorrelation,  $p < 10^{-4}$ ) than those based on all  
 356 nodes. The early warning signals based on the High Input nodes improved over those based on all  
 357 nodes ( $p < 10^{-4}$  for all the early warning signals except the maximum standard deviation, for which  
 358  $p = 0.025$ ) on average but were not as good as those based on the Lower State nodes in the case  
 359 of the average standard deviation (High Input:  $\tau = 0.873$ , Lower State:  $\tau = 0.883$ ). The  $\tau$  values  
 360 at most moderately depended on the network structure. Specifically, the distribution of random  
 361 intercepts for network had the smallest standard deviation in the estimated linear mixed effects  
 362 models for the maximum standard deviation early warning signal (0.022, 2.7% of the magnitude  
 363 of the intercept) and the largest standard deviation for the average autocorrelation early warning  
 364 signal (0.041, 6.2%). These results are consistent with and generalize in terms of the variety of  
 365 networks those shown in Fig. 2.

366 We then investigated the robustness of the results shown in Fig. 2 against changes in parameter  
 367 values. The full results are shown in the SI (see section S10). Consistent with previous results  
 368 (e.g., [32]), decreasing the number of samples for calculating the early warning signal,  $M$ , has the  
 369 strongest negative effect on the performance of early warning signals. We have also found that  
 370 the average standard autocorrelation calculated from all nodes tends to perform worse than that  
 371 calculated from the other node sets when the double-well equilibrium points are relatively close  
 372 together (i.e.,  $(r_1, r_2, r_3) = (1, 3, 5)$  as opposed to  $(1, 4, 7)$ ) or  $r_1$ ,  $r_2$ , and  $r_3$  are not evenly spaced  
 373 (i.e.,  $(r_1, r_2, r_3) = (1, 2.5, 7)$  or  $(1, 5.5, 7)$  as opposed to  $(1, 4, 7)$ ). As expected, allowing more than  
 374 50 TU for the model to relax to an equilibrium does not markedly improve the performance of the  
 375 early warning signals. Thus, with the notable exception of the effect of  $M$ , the performance of  
 376 each early warning signal is in general fairly similar across the different parameter settings.

### 377 C. When We Do Not Know the Network Structure

378 When we do not know the network structure, we cannot calculate  $R_i$ , which uses the adjacency  
 379 matrix, to identify High Input nodes. Therefore, we explored the use of a correlation-based index,

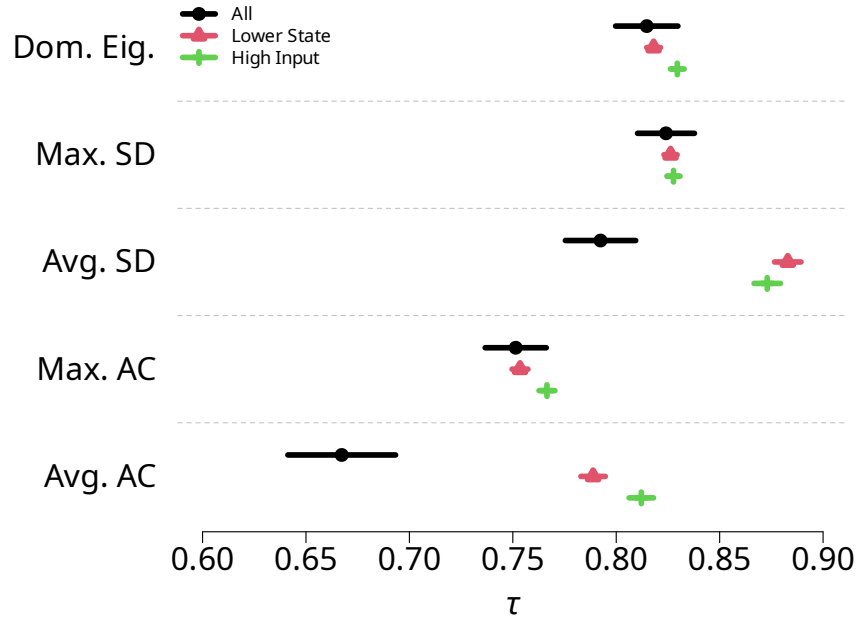


FIG. 3. Predicted Kendall correlations ( $\tau$ ) for five early warning signals and three node sets, estimated by a linear mixed effects model with a fixed effect for node set and a random effect for network. The results are based on the ten networks that have multiple stable ranges of  $D$  in our numerical simulations. Markers (All: circles, Lower State: triangles, High Input: pluses) signify the predicted  $\tau$  value. The horizontal lines represent the 95% confidence intervals.

380  $R'_i$  (see section IID for the definition), to choose alternative sentinel nodes, called the Large Cor-  
 381 relation nodes, and computed the same set of early warning signals. We show the results for the  
 382 Large Correlation node set by the box-times symbols in Fig. 2. The Large Correlation node set  
 383 performed worse than the High Input node set. This result is expected because High Input uses  
 384 the information about the network structure, whereas Large Correlation does not. However, the  
 385 Large Correlation node set performed better than the Lower Half and Random node sets. In fact,  
 386  $\tau$  with the Large Correlation node set is reasonably large in the dolphin network, roughly ranging  
 387 between 0.6 and 0.8, whereas it is low in the power-law network (i.e.,  $\tau < 0.5$ ). The discrepancy  
 388 between the results for the two networks is associated with the different fidelity with which the  
 389 Pearson correlation matrix,  $\text{cor}(x_i, x_j)$ , reflects the actual adjacency matrix (see Fig. S9).

390 We also considered the nodes with the largest standard deviation in  $x_i$ , called Large SD, as  
 391 another node set that does not need the information about the network structure. The rationale  
 392 behind Large SD is that, when the  $i$ th node receives large input from other nodes, i.e., when  $R_i$  is  
 393 large, the standard deviation of  $R_i$  should also be large because each  $x_j$  in Eq. (1) is fluctuating due  
 394 to dynamical noise. A large fluctuation in  $R_i$  is expected to make the standard deviation of  $x_i$  large

395 through Eq. (1). We found that early warning signals based on Large SD nodes (shown by stars in  
 396 Fig. 2) perform better than those based on Large Correlation nodes and that the Large SD node  
 397 set is approximately as well as the High Input node set. Both the Large SD and, to a lesser extent,  
 398 the Large Correlation node sets perform well even when we consider all node transitions, not just  
 399 those occurring after a stable range (Fig S8). However, the Large SD node set is particularly  
 400 sensitive to the number of samples used to determine node membership; its performance declines  
 401 substantially on this test when we use only the first ten samples to determine node membership  
 402 (Fig. S7).

403 Overall, these results support the idea of network-aware choice of sentinel nodes for early warning  
 404 multistage transitions even when we do not have connectivity data at hand.

#### 405 **D. Transition from the Upper State to the Lower State**

406 Simulations of Eq. (2) on the power-law and dolphin networks with all nodes beginning in the  
 407 upper state also show multistate transitions (see Fig S10). With Eq. (2), high-degree nodes receive  
 408 a large positive contribution from the coupling term, which is the same as with Eq. (1). Therefore,  
 409 lower-degree nodes or those adjacent to fewer upper-state nodes are most likely to transition from  
 410 the upper to the lower state when  $D$  gradually decreases. For this reason, Lower State and High  
 411 Input, which are two node sets that performed well when we attempted to anticipate transition  
 412 from the lower to upper states, are not expected to be equally good sentinels when the tipping  
 413 direction is reversed, that is, when the system begins with nodes at the upper state and transits  
 414 to the lower state. Therefore, we additionally considered two node sets that are mirror images  
 415 of Lower State and High Input. One is the set of nodes in the upper state, which we already  
 416 considered in Fig. 2. The other is Low Input, which is the  $n$  nodes with the smallest  $R_i$  among the  
 417 upper-state nodes; they are candidate of nodes that may transit from the upper to the lower state  
 418 earlier than other nodes as  $D$  decreases.

419 We show the Kendall's  $\tau$  for the power-law and dolphin networks in Fig. 4. In Fig. 4, a negative  
 420  $\tau$  indicates that the early warning signal became large as  $D$  decreased towards a transition from the  
 421 upper to the lower state. Therefore, large negative  $\tau$  values are indicative of critical slowing down  
 422 as we decrease  $D$ . We find that the early warning signals calculated from lower-state nodes (Lower  
 423 State, shown by the triangles, and High Input, shown by pluses) are not useful for anticipating  
 424 transitions. In contrast, those calculated from the All node set (shown by the circles) or those  
 425 informed by upper-state node dynamics (Upper State, shown by crosses; Low Input, shown by



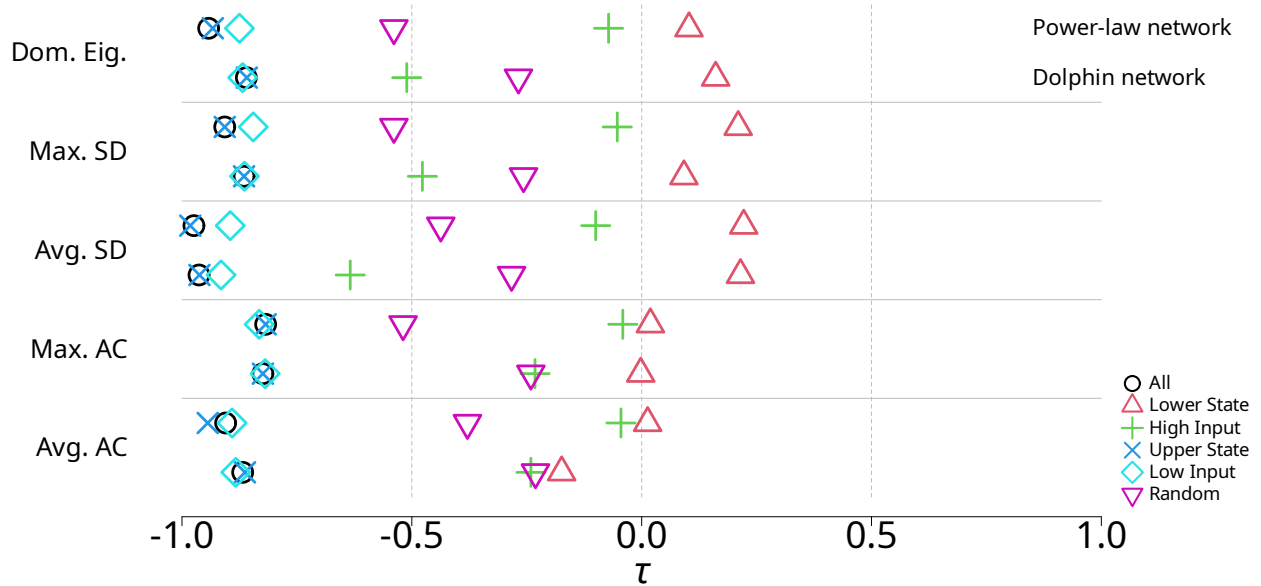


FIG. 4. Early warning signals in multistage transitions from the upper to lower equilibria. Kendall correlations ( $\tau$ ) between each of the five early warning signals and the coupling strength,  $D$ , for different sets of nodes when the dynamics begin with the nodes in the upper state and  $D$  gradually decreases are shown. See the caption of Fig. 2 for the abbreviation of the early warning signals.

426 diamonds) are highly negatively correlated with  $D$ . This result indicates that the nodes in the  
 427 upper state, not those in the lower state, provide useful early warning signals. Furthermore, the  
 428 best sentinel nodes are opposite in terms of  $R_i$  from when we started with the lower equilibrium  
 429 and observed transitions of the nodes from the lower to the upper state. A suitable choice of  
 430 sentinel nodes depends on the tipping direction, even if the dynamical system model is similar or  
 431 essentially the same.

432

#### IV. DISCUSSION

433 We showed that both multivariate (i.e., eigenvalue-based) and aggregated univariate (i.e.,  
 434 variance- and autocorrelation-based) early warning signals can provide advance notice of state  
 435 changes in multistage transitions in coupled double-well systems. Furthermore, we showed that  
 436 constructing early warning signals only based on a subset of nodes, called sentinel nodes, is com-  
 437 petitive with, and sometimes more effective than, using all nodes to calculate the early warning  
 438 signals. Specifically, it is useful to monitor nodes that have not transitioned to the alternative  
 439 state but are connected to other nodes that have already transitioned to such a state. We showed

440 that the early warning signals calculated based on the thus selected sentinel nodes were effective  
 441 both when nodes were transitioning from a lower state to an upper state and vice versa. Up to  
 442 our numerical efforts, the results were robust against parameter variation, network structure, and  
 443 choice of early warning signals.

444 We have shown that the choice of which nodes to monitor for early warning signals has a marked  
 445 impact on the effectiveness of the early warning signal. In particular, when we observed transitions  
 446 from the lower to upper states, a good set of nodes to monitor was those with a large degree or with  
 447 many connections to other nodes that have already transitioned to the upper state, as quantified by  
 448  $R_i$ . At first glance, this result seems at odds with those by Aparicio et al. [14], who used network  
 449 control theory to propose that lower-degree nodes tended to make better sentinels. In fact, in their  
 450 model, the dynamics always starts with nodes in the upper state because it is a model of species  
 451 abundance and its loss. We showed that lower-degree nodes are good sentinel nodes when the  
 452 nodes are initially in their upper states and transit to their lower states as a bifurcation parameter  
 453 gradually changes. Aparicio et al. provided two indices for the suitability of their sentinel nodes.  
 454 Because one of the two indices only depends on the network structure, we calculated the other  
 455 measure, called  $\rho$ , for our simulations given the network. A value of  $\rho$  closer to zero indicates that  
 456 their sentinel nodes are more suitable. We found for our power-law network  $\rho = 0.042$  when all  
 457 nodes start in the lower state and  $\rho = 0.038$  when all nodes start in the upper state; for the dolphin  
 458 network, we obtained  $\rho = 0.030$  and  $\rho = 0.007$ , respectively. These results are consistent with our  
 459 numerical results, in which low-degree nodes provide informative early warning signals when we  
 460 started with the upper but not the lower state. We emphasize that a good choice of sentinel nodes  
 461 depends on the initial condition and the tipping direction even if we fix the dynamical system as  
 462 well as the network structure.

463 There are many cases in which a network model is thought to represent a complex system  
 464 showing tipping phenomena but the edges of the network are not directly known [33]. Examples  
 465 include the co-occurrence of symptoms of neurological conditions [34] and the rates of return  
 466 on traded financial securities [35]. In such cases, we are typically given only multivariate time  
 467 series data and want to derive informative early warning signals for tipping points that possibly  
 468 constitute a multistage transition. A strategy in this situation is to infer the network structure from  
 469 multivariate time series data [33, 36] and then calculate candidate sentinel nodes from the estimated  
 470 network using, for example, the node's ranking in terms of  $R_i$ . We avoided this approach because  
 471 network inference from time series data is subject to error due to, e.g., thresholding decisions [33] or  
 472 uncertainty in model estimation [36]. Instead, we proposed a method to identify sentinel nodes only

473 based on the Pearson correlation between the time series at pairs of nodes, which provides a proxy  
474 to edges (although one should not use the Pearson correlation as an estimate of the network edge in  
475 general [37]). Our sentinel nodes determined based on the Pearson correlation provided reasonably  
476 strong early warning signals, but their performance did not reach that for the case in which we  
477 know the network structure. However, choosing sentinel nodes based on the standard deviation  
478 of the node's state performed in a similar manner to sentinel nodes chosen using information on  
479 network structure. Finding better sentinel nodes given multivariate time series data for which the  
480 explicit network structure is unknown warrants future work. We also point out that we currently  
481 do not have equivalent methods when the nodes are initially in their upper states and transit to  
482 their lower states as the value of a control parameter gradually varies, which is typical in ecological  
483 modeling.

484 Although we have shown that High and Low Input node sets are efficient at anticipating major  
485 changes of state in the models we studied, there is much room for further improvements. First,  
486 multistage transitions imply that there are intermediate stages in which some nodes have tipped  
487 and the others have not and that we have seen a history of which nodes have tipped and when. If  
488 we use such information, we may be able to improve performances of early warning signals with  
489 respect to both the node set selection and the definition of the signal. Second, it may be helpful  
490 to use benchmark networks that show multistage transitions. If a network is composed of multiple  
491 disconnected components of tipping elements, the entire network should show multistage transitions  
492 because the different disconnected components show a bifurcation at different values of a control  
493 parameter in general. Therefore, a network with a strong planted community structure is expected  
494 to show multistage transitions for various dynamical systems. Degree-heterogeneous random graphs  
495 also show multistage transitions, which is underpinned by both numerical simulations and a mean  
496 field theory [20]. Studying multistage transitions and early warning signals on these networks may  
497 be useful.

498 We used cubic polynomials to drive the node's dynamics (and hence a potential in the form  
499 of quartic polynomials) and unipartite networks to test our ideas. These modeling assumptions  
500 are reasonable for investigating, for example, climate and vegetation cover transitions [38, 39].  
501 In contrast, various ecological systems are better modeled by bipartite networks, in which the  
502 two layers of nodes typically represent pollinators (or seed dispersers) and plants [12, 40]. In  
503 fact, ecological dynamics on bipartite networks also show multistage transitions [12]. Despite the  
504 seminal work based on network control theory [14], discussed above, further work is desirable for  
505 identifying informative sentinel nodes in ecological dynamics on bipartite networks. Other types of

506 dynamics such as reactive and synchronization dynamics on networks should also be investigated.  
 507 Additionally, although saddle-node bifurcations have been frequently studied, natural systems may  
 508 also show other types of bifurcations. Early warning signals for transcritical, Hopf, and other  
 509 bifurcations are beyond the scope of this work, but anticipating such transitions is important in  
 510 several fields, including the epidemiology [41] and ecology [12]. Finally, although we have shown  
 511 that a careful choice of sentinel nodes can dramatically reduce the amount of data needed without  
 512 sacrificing the quality of early warning signals, we are ignorant of the amount of the data needed  
 513 from each node in this study. Shortening the length of temporal data required will be an important  
 514 next step, given that sampling can be expensive and invasive in various applications such as ecology  
 515 and medicine. Spatial correlations such as Moran’s  $I$  have been used to provide early warning  
 516 signals on square lattices [42], and their extensions to the case of complex networks may help  
 517 reduce the required amount of temporal sampling.

518 In addition to sampling limitations, the specificity of early warning signals is a known challenge  
 519 [43–46]. Suppose that an early warning signal tends to increase as a control parameter gradually  
 520 increases towards a tipping point. It is difficult in general, however, to suggest a particular range of  
 521 values of the early warning signal that indicates an impending transition. In fact, the Kendall’s  $\tau$ ,  
 522 which is deemed to be a standard performance measure, may be large for several reasons, including  
 523 when the early warning signal monotonically increases as the control parameter increases regardless  
 524 of tipping points [44]. This lack of specificity is also present in our results (see Fig. 1). Developing  
 525 methods, such as maximum likelihood [44] or algorithmic classification [45] techniques, to improve  
 526 the specificity of early warning signals is an important area of further research. With all these tasks  
 527 saved for future work, by combining information about the network structure and dynamics, the  
 528 present study takes a significant step towards accurately and cost-efficiently anticipating different  
 529 types of tipping points in complex dynamical systems.

530

#### DATA ACCESSIBILITY

531 The datasets generated and analyzed during the current study are available in the GitHub  
 532 repository, <https://github.com/ngmaclaren/doublewells>, along with all relevant computer code.

533

#### ACKNOWLEDGMENTS

534 We thank Hiroshi Kori and Makito Oku for valuable discussion.

535 **AUTHOR CONTRIBUTIONS**

536 N.M. conceived and supervised the project. N.G.M. performed the simulations and computa-  
537 tions with assistance from P.K.. N.G.M. and N.M. analyzed the data and wrote the paper.

538 **FUNDING**

539 N. Masuda acknowledges support from AFOSR European Office (under Grant No. FA9550-19-  
540 1-7024), the Sumitomo Foundation, the Japan Science and Technology Agency (JST) Moonshot  
541 R&D (under Grant No. JPMJMS2021), and the National Science Foundation (under Grant No.  
542 2052720).

543 **CONFLICT OF INTEREST DECLARATION**

544 The authors declare no competing interests.

- 
- 545 [1] Marten Scheffer, S Harry Hosper, Marie-Louise Meijer, Brian Moss, and Erik Jeppesen. Alternative  
546 equilibria in shallow lakes. *Trends in Ecology & Evolution*, 8(8):275–279, 1993.
- 547 [2] Stephen R Carpenter, Jonathan J Cole, Michael L Pace, Ryan Batt, William A Brock, Timmothy  
548 Cline, Jim Coloso, James R Hodgson, Jim F Kitchell, David A Seekell, et al. Early warnings of regime  
549 shifts: a whole-ecosystem experiment. *Science*, 332(6033):1079–1082, 2011.
- 550 [3] Philip C Reid, Renata E Hari, Grégory Beaugrand, David M Livingstone, Christoph Marty, Dietmar  
551 Straile, Jonathan Barichivich, Eric Goberville, Rita Adrian, Yasuyuki Aono, et al. Global impacts of  
552 the 1980s regime shift. *Global Change Biology*, 22(2):682–703, 2016.
- 553 [4] Jose G Venegas, Tilo Winkler, Guido Musch, Marcos F Vidal Melo, Dominick Layfield, Nora  
554 Tgavalekos, Alan J Fischman, Ronald J Callahan, Giacomo Bellani, and R Scott Harris. Self-organized  
555 patchiness in asthma as a prelude to catastrophic shifts. *Nature*, 434(7034):777–782, 2005.
- 556 [5] Jerome Clifford Foo, Hamid Reza Noori, Ikuhiro Yamaguchi, Valentina Vengeliene, Alejandro Cosa-  
557 Linan, Toru Nakamura, Kenji Morita, Rainer Spanagel, and Yoshiharu Yamamoto. Dynamical state  
558 transitions into addictive behaviour and their early-warning signals. *Proceedings of the Royal Society  
559 B: Biological Sciences*, 284(1860):20170882, 2017.
- 560 [6] Marten Scheffer, Jordi Bascompte, William A Brock, Victor Brovkin, Stephen R Carpenter, Vasilis  
561 Dakos, Hermann Held, Egbert H Van Nes, Max Rietkerk, and George Sugihara. Early-warning signals  
562 for critical transitions. *Nature*, 461(7260):53–59, 2009.

- 563 [7] Lei Dai, Daan Vorselen, Kirill S Korolev, and Jeff Gore. Generic indicators for loss of resilience before  
564 a tipping point leading to population collapse. *Science*, 336(6085):1175–1177, 2012.
- 565 [8] Paul DH Hines, Eduardo Cotilla-Sanchez, Benjamin O’hara, and Christopher Danforth. Estimating  
566 dynamic instability risk by measuring critical slowing down. In *2011 IEEE Power and Energy Society  
567 General Meeting, Detroit, MI*, page 12303648, New York, NY, 2011. IEEE.
- 568 [9] Michael L Pace, Ryan D Batt, Cal D Buelo, Stephen R Carpenter, Jonathan J Cole, Jason T Kurtzweil,  
569 and Grace M Wilkinson. Reversal of a cyanobacterial bloom in response to early warnings. *Proceedings  
570 of the National Academy of Sciences of the United States of America*, 114(2):352–357, 2017.
- 571 [10] Thilo Gross and Bernd Blasius. Adaptive coevolutionary networks: a review. *Journal of the Royal  
572 Society Interface*, 5(20):259–271, 2008.
- 573 [11] Xueming Liu, Daqing Li, Manqing Ma, Boleslaw K Szymanski, H Eugene Stanley, and Jianxi Gao.  
574 Network resilience. *Physics Reports*, 971:1–108, 2022.
- 575 [12] J Jelle Lever, Ingrid A van de Leemput, Els Weinans, Rick Quax, Vasilis Dakos, Egbert H van Nes, Jordi  
576 Bascompte, and Marten Scheffer. Foreseeing the future of mutualistic communities beyond collapse.  
577 *Ecology Letters*, 23(1):2–15, 2020.
- 578 [13] Vasilis Dakos. Identifying best-indicator species for abrupt transitions in multispecies communities.  
579 *Ecological Indicators*, 94:494–502, 2018.
- 580 [14] Andrea Aparicio, Jorge X Velasco-Hernández, Claude H Moog, Yang-Yu Liu, and Marco Tulio Angulo.  
581 Structure-based identification of sensor species for anticipating critical transitions. *Proceedings of the  
582 National Academy of Sciences of the United States of America*, 118(51):e2104732118, 2021.
- 583 [15] J Jelle Lever, Egbert H van Nes, Marten Scheffer, and Jordi Bascompte. The sudden collapse of  
584 pollinator communities. *Ecology Letters*, 17(3):350–359, 2014.
- 585 [16] Vasilis Dakos and Jordi Bascompte. Critical slowing down as early warning for the onset of collapse  
586 in mutualistic communities. *Proceedings of the National Academy of Sciences of the United States of  
587 America*, 111(49):17546–17551, 2014.
- 588 [17] Jianxi Gao, Baruch Barzel, and Albert-László Barabási. Universal resilience patterns in complex net-  
589 works. *Nature*, 530(7590):307–312, 2016.
- 590 [18] Nico Wunderling, Maximilian Gelbrecht, Ricarda Winkelmann, Jürgen Kurths, and Jonathan F Donges.  
591 Basin stability and limit cycles in a conceptual model for climate tipping cascades. *New Journal of  
592 Physics*, 22(12):123031, 2020.
- 593 [19] Prosenjit Kundu, Hiroshi Kori, and Naoki Masuda. Accuracy of a one-dimensional reduction of dy-  
594 namical systems on networks. *Physical Review E*, 105(2):024305, 2022.
- 595 [20] Prosenjit Kundu, Neil G MacLaren, Hiroshi Kori, and Naoki Masuda. Mean-field theory for double-well  
596 systems on degree-heterogeneous networks. *Proceedings of the Royal Society A: Mathematical, Physical,  
597 and Engineering Sciences*, 478:20220350, 2022.
- 598 [21] Leo Lahti, Jarkko Salojärvi, Anne Salonen, Marten Scheffer, and Willem M de Vos. Tipping elements  
599 in the human intestinal ecosystem. *Nature Communications*, 5(1):4344, 2014.

- 600 [22] Charles D Brummitt, George Barnett, and Raissa M D'Souza. Coupled catastrophes: sudden shifts cas-  
601 cade and hop among interdependent systems. *Journal of The Royal Society Interface*, 12(112):20150712,  
602 2015.
- 603 [23] Els Weinans, Rick Quax, Egbert H van Nes, and Ingrid A van de Leemput. Evaluating the performance  
604 of multivariate indicators of resilience loss. *Scientific Reports*, 11(1):9148, 2021.
- 605 [24] Luonan Chen, Rui Liu, Zhi-Ping Liu, Meiyi Li, and Kazuyuki Aihara. Detecting early-warning signals  
606 for sudden deterioration of complex diseases by dynamical network biomarkers. *Scientific Reports*,  
607 2(1):342, 2012.
- 608 [25] Vasilis Dakos, Stephen R Carpenter, William A Brock, Aaron M Ellison, Vishwesh Guttal, Anthony R  
609 Ives, Sonia Kefi, Valerie Livina, David A Seekell, Egbert H van Nes, et al. Methods for detecting early  
610 warnings of critical transitions in time series illustrated using simulated ecological data. *PloS ONE*,  
611 7(7):e41010, 2012.
- 612 [26] Vasilis Dakos, Marten Scheffer, Egbert H van Nes, Victor Brovkin, Vladimir Petoukhov, and Hermann  
613 Held. Slowing down as an early warning signal for abrupt climate change. *Proceedings of the National  
614 Academy of Sciences of the United States of America*, 105(38):14308–14312, 2008.
- 615 [27] David Lusseau, Karsten Schneider, Oliver J Boisseau, Patti Haase, Elisabeth Slooten, and Steve M  
616 Dawson. The bottlenose dolphin community of doubtful sound features a large proportion of long-  
617 lasting associations. *Behavioral Ecology and Sociobiology*, 54(4):396–405, 2003.
- 618 [28] Gabor Csardi and Tamas Nepusz. The igraph software package for complex network research. *Inter-  
619 Journal, Complex Systems*:1695, 2006.
- 620 [29] Jose Pinheiro, Douglas Bates, Saikat DebRoy, Deepayan Sarkar, and R Core Team. *nlme: Linear and  
621 Nonlinear Mixed Effects Models*, 2021. R package version 3.1-153.
- 622 [30] R Core Team. *R: A Language and Environment for Statistical Computing*. R Foundation for Statistical  
623 Computing, Vienna, Austria, 2022.
- 624 [31] David Schoch. *networkdata: Repository of Network Datasets*, 2022. R package version 0.1.10.
- 625 [32] Christopher F Clements, John M Drake, Jason I Griffiths, and Arpat Ozgul. Factors influencing the  
626 detectability of early warning signals of population collapse. *American Naturalist*, 186(1):50–58, 2015.
- 627 [33] Ivan Brugere, Brian Gallagher, and Tanya Y Berger-Wolf. Network structure inference, a survey:  
628 Motivations, methods, and applications. *ACM Computing Surveys*, 51(2):24, 2018.
- 629 [34] Stefan G Hofmann, Joshua Curtiss, and Richard J McNally. A complex network perspective on clinical  
630 science. *Perspectives on Psychological Science*, 11(5):597–605, 2016.
- 631 [35] Rick Quax, Drona Kandhai, and Peter M A Sloot. Information dissipation as an early-warning signal  
632 for the lehman brothers collapse in financial time series. *Scientific Reports*, 3(1):1898, 2013.
- 633 [36] Marc Timme and Jose Casadiego. Revealing networks from dynamics: an introduction. *Journal of  
634 Physics A: Mathematical and Theoretical*, 47(34):343001, 2014.
- 635 [37] Andrew Zalesky, Alex Fornito, and Ed Bullmore. On the use of correlation as a measure of network  
636 connectivity. *NeuroImage*, 60(4):2096–2106, 2012.

- 637 [38] Nico Wunderling, Jonathan F Donges, Jürgen Kurths, and Ricarda Winkelmann. Interacting tip-  
638 ping elements increase risk of climate domino effects under global warming. *Earth System Dynamics*,  
639 12(2):601–619, 2021.
- 640 [39] Nico Wunderling, Arie Staal, Boris Sakschewski, Marina Hirota, Obbe A. Tuinenburg, Jonathan F.  
641 Donges, Henrique M. J. Barbosa, and Ricarda Winkelmann. Recurrent droughts increase risk of cas-  
642 cading tipping events by outpacing adaptive capacities in the amazon rainforest. *Proceedings of the*  
643 *National Academy of Sciences of the United States of America*, 119(32):e2120777119, 2022.
- 644 [40] Jordi Bascompte and Pedro Jordano. Plant-animal mutualistic networks: the architecture of biodiver-  
645 sity. *Annual Review of Ecology, Evolution, and Systematics*, 38:567–593, 2007.
- 646 [41] John M Drake, Tobias S Brett, Shiyang Chen, Bogdan I Epureanu, Matthew J Ferrari, Éric Marty,  
647 Paige B Miller, Eamon B O’dea, Suzanne M O’regan, Andrew W Park, et al. The statistics of epidemic  
648 transitions. *PLoS Computational Biology*, 15(5):e1006917, 2019.
- 649 [42] Vasilis Dakos, Egbert H van Nes, Raúl Donangelo, Hugo Fort, and Marten Scheffer. Spatial correlation  
650 as leading indicator of catastrophic shifts. *Theoretical Ecology*, 3(3):163–174, 2010.
- 651 [43] Alena Sonia Gsell, Ulrike Scharfenberger, Deniz Özkundakci, Annika Walters, Lars-Anders Hansson,  
652 Annette BG Janssen, Peeter Nõges, Philip C Reid, Daniel E Schindler, Ellen Van Donk, et al. Evaluating  
653 early-warning indicators of critical transitions in natural aquatic ecosystems. *Proceedings of the National*  
654 *Academy of Sciences of the United States of America*, 113(50):E8089–E8095, 2016.
- 655 [44] Carl Boettiger and Alan Hastings. Quantifying limits to detection of early warning for critical transi-  
656 tions. *Journal of the Royal Society Interface*, 9(75):2527–2539, 2012.
- 657 [45] Thomas M Bury, RI Sujith, Induja Pavithran, Marten Scheffer, Timothy M Lenton, Madhur Anand,  
658 and Chris T Bauch. Deep learning for early warning signals of tipping points. *Proceedings of the*  
659 *National Academy of Sciences of the United States of America*, 118(39):e2106140118, 2021.
- 660 [46] Maarten C Boerlijst, Thomas Oudman, and André M de Roos. Catastrophic collapse can occur without  
661 early warning: examples of silent catastrophes in structured ecological models. *PLoS ONE*, 8(4):e62033,  
662 2013.